3270 *Chem. Mater.* **2009,** *21,* 3270–3274
DOI:10.1021/cm900786s

CHEMISTRY OF MATERIALS
Article

Nucleotide-Based Templates for Nanoparticle Production−Exploiting Multiple Noncovalent Interactions

Mei Li,[†] Richard J. Oakley,[†] Harry Bevan,[†] Bernd M. Smarsly,[‡] Stephen Mann,[†] and Charl F.J. Faul*[,†]

[†]*Inorganic and Materials Chemistry, School of Chemistry, University of Bristol, Bristol BS8 1TS, United Kingdom, and* [‡]*Institute of Physical Chemistry, University of Giessen, Heinrich-Buff-Ring 58, D-35392 Giessen, Germany*

Received March 20, 2009. Revised Manuscript Received June 1, 2009

We demonstrate that complex functional nanomaterials based on stacked metal ion-containing G quadruplexes and cationic surfactant self-assembly can be readily fabricated. Specifically, we show that multiple noncovalent interactions can be utilized to construct well-organized thermotropic LC materials, which can be subsequently exploited for the production of complex materials comprising Ag nanoparticles.

The guanosine moiety has recently received considerable attention not only for its ability to form self-complementary hydrogen-bonding structures,[1,2] but also for its prominence and relevance to control mechanisms in cancer-related cell biology.[3,4] We are interested in exploring the potential of the guanosine moiety to generate intricate G-quartet motifs and stacked G-quadruplex superstructures[5] for applications in the programmed design of complex functional materials.[6,7] In this regard, G-quartet-forming nucleotides are attractive building blocks for molecular materials as they self-associate through hydrogen bonding, undergo metal ion-mediated quadruplex stacking by cation-dipole interactions,[8] and self-organize into longer range structures by noncovalent interactions involving the peripheral phosphate groups.[9] Based on these capabilities, guanosine derivatives have been used in a number of materials-related investigations, including the formation of micrometric helices,[10] cholesteric lyotropic phases,[11] constitutional dynamic gelations and selection,[12,13] nanoparticle assembly,[14] and the construction of complex hierarchical materials.[15]

Control of the interplay and balance of forces and interactions in synthetic assemblies comprising multiple motifs is critically important for the regulation of growth and structure formation. Recently, we demonstrated this by exploiting the multiple noncovalent interactions associated with the G-quartet motif for the production of complex self-organizing nanostructures.[9,15] Although the control of nanostructure architectures appears to be amenable to rational design, the ability to incorporate functionality and switchability/reversibility in G-quartet-derived nanostructures remains a key challenge. In this respect, we herein present a novel approach in which electrostatic coassembly of a stacked metal ion-containing G-quadruplex in the presence of a cationic surfactant is used for the preparation of nucleotide-based thermotropic liquid-crystalline materials. We make use of Hoogsteen hydrogen bonding, π-stacking, and cation-dipole interactions to assemble and stabilize supramolecular stacks of K^+- or Ag^+-containing 2′-deoxyguanosine 5′-monophosphate (dGMP) quartets (Scheme 1).

Once formed, we use the polyanionic array associated with the stacked phosphate moieties of dGMP for the ionic self-assembly[16] of oppositely charged dialkyldimethylammonium bromide surfactants with variable chain length (DiC_n; n = 10, 12, 14, 16). This second assembly step leads to the production of complex G-quadruplex nanostructures (G4-DiC_n) exhibiting thermotropic liquid crystal properties. Thermotropic phase behavior has been shown previously for covalently

*Corresponding author. E-mail: charl.faul@bristol.ac.uk. Fax: (44) 117-929-0509. Tel: (44) 117-954-6321.

(1) Davis, J. T. *Angew. Chem., Int. Ed.* **2004**, *43*, 668–698.
(2) Davis, J. T.; Spada, G. P. *Chem. Soc. Rev.* **2007**, *36*, 296–313.
(3) Oganesian, L.; Bryan, T. M. *Bioessays* **2007**, *29*, 155–165.
(4) Bugaut, A.; Jantos, K.; Wietor, J.-L.; Rodriguez, R.; Sanders, J. K. M.; Balasubramanian, S. *Angew. Chem., Int. Ed.* **2008**, *47*, 2677–2680.
(5) Gellert, M.; Lipsett, M. N.; Davies, D. R. *Proc. Natl. Acad. Sci. U. S.A.* **1962**, *48*, 2013.
(6) Lehn, J. M. *Proc. Natl. Acad. Sci. U.S.A.* **2002**, *99*, 4763–4768.
(7) Bromley, E. H. C.; Channon, K.; Moutevelis, E.; Woolfson, D. N. *ACS Chem. Biol.* **2008**, *3*, 38–50.
(8) Pinnavaia, T. J.; Marshall, C. L.; Mettler, C. M.; Fisk, C. I.; Miles, H. T.; Becker, E. D. *J. Am. Chem. Soc.* **1978**, *100*, 3625–3627.
(9) Ozer, B. H.; Smarsly, B.; Antonietti, M.; Faul, C. F. J. *Soft Matter* **2006**, *2*, 329–336.
(10) Aime, C.; Manet, S.; Satoh, T.; Ihara, H.; Park, K. Y.; Godde, F.; Oda, R. *Langmuir* **2007**, *23*, 12875–12885.
(11) Gottarelli, G.; Spada, G. P. *Chem. Rec.* **2004**, *4*, 39–49.
(12) Ghoussoub, A.; Lehn, J. M. *Chem. Commun.* **2005**, 5763–5765.
(13) Sreenivasachary, N.; Lehn, J. M. *Proc. Natl. Acad. Sci. U.S.A.* **2005**, *102*, 5938–5943.
(14) Li, Z.; Mirkin, C. A. *J. Am. Chem. Soc.* **2005**, *127*, 11568–11569.
(15) Houbenov, N.; Nykanen, A.; Iatrou, H.; Ruokolainen, J.; Hadjichristidis, N.; Faul, C. F. J.; Ikkala, I. *Adv. Funct. Mater.* **2008**, *18*, 2041–2047.
(16) Faul, C. F. J.; Antonietti, M. *Adv. Mater.* **2003**, *15*, 673–683.

Published on Web 06/29/2009

Scheme 1. Schematic Representation of the Assembly and Use of the G-Quartet-Surfactant Templates

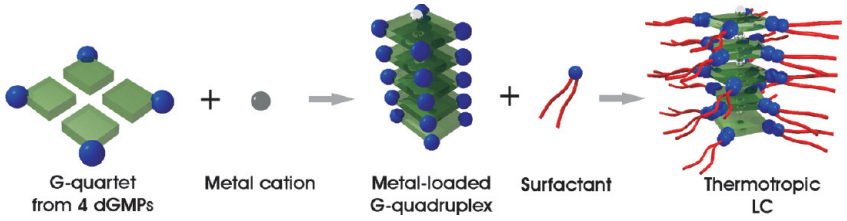

modified folic acid derivatives.[17] We then exploit the preorganization of Ag^+ ions in the nucleotide-surfactant liquid crystal for the fabrication of well-defined ordered arrays of silver nanoparticles within the dGMP matrix. The use of ionic self-assembly to produce novel types of G-quadruplex nanocomposites and soft templates with controlled architecture should provide insight and understanding into the use of dGMP and related motifs for producing complex functional materials, and help elucidate the interactions and synthetic protocols necessary to manipulate biorelevant motifs for materials applications.

Experimental Section

Materials. 2′-Deoxyguanosine 5′-monophosphate (dGMP) sodium salt hydrate and potassium chloride were purchased from Sigma. The ammonium bromide surfactants didecyldimethyl ammonium bromide (DiC_{10}), didodecyldimethyl ammonium bromide (DiC_{12}), ditetradecyldimethyl ammonium bromide (DiC_{14}), and dihexadecyldimethyl ammonium bromide (DiC_{16}) were obtained from Fluka. All materials were used without further purification.

Preparation of K^+-G4-Surfactant Complexes. dGMP powder was dissolved in KCl aqueous solution (0.1 M, pH 5.2) to give a concentration of dGMP of 0.2 M. The resultant clear solution was incubated at 4 °C for 3−5 days to ensure formation of G-quartet or G-quadruplex structures. The G-quartet (dGMP-K^+) solution was slowly added with gentle shaking to an aqueous solution containing an ammonium bromide surfactant (0.1 M) at a dGMP:surfactant molar ratio of 1:1. The mixture was incubated at room temperature overnight, and the G4-quadruplex-surfactant precipitate collected by centrifugation and then washed three times with water. After being dried under a vacuum, the product was dissolved in chloroform and then redried under a vacuum.

Preparation of Ag^+-G4-Surfactant Complexes and Ag Nanoparticle Composites. dGMP powder was dissolved in $AgNO_3$ aqueous solution (0.05 M, pH 5.2) to give a concentration of dGMP of 0.2 M and molar ratio of dGMP to Ag^+ of 4:1. The resultant clear solution was incubated at 23 °C for 48 h protected from light to avoid Ag photoreduction and to ensure the formation of G-quartet or G-quadruplex structures. The G-quartet (dGMP-Ag^+) solution was then slowly added with gentle shaking to an aqueous solution of didodecyldimethylammonium bromide (DiC_{12}) surfactant (0.1 M) at the molar ratio of dGMP to surfactant of 1:1, which generated a white gel-like solution. After incubation at 4 °C for 24 h, the mixture (in a 1.5 mL plastic centrifuge tube) was exposed to a 345 nm UV lamp for 2 h. No color change was observed. The G4-quadruplex-Ag-surfactant complex was collected by centrifugation and then washed three times with water. After drying under a vacuum, the product was dissolved in dichloromethane and analyzed.

Preparation of Samples for TEM and AFM Investigations. Samples for transmission electron microscopy (TEM) were prepared by depositing 3 μL $CHCl_3$ solution of K^+-G-quartet-surfactant chloroform solution onto carbon-coated 3-mm-diameter, copper electron microscope grids, and allowing the sample to dry in air. Where the samples were stained, 2 μL of uranyl acetate (1%) solution was applied to the grid.

Samples for AFM investigations were diluted to 1 mg/mL, drop casted, and dried onto freshly cleaved mica. Imaging was in air at ambient temperature.

Instrumentation. Wide-angle X-ray scattering (WAXS) measurements were performed at the Hamburg Synchrotronstrahlungslabor HASYLAB at DESY, Beamline A2. A semicrystalline PET sample was used as calibration standard. Small-angle X-ray scattering (SAXS) was done at room temperature using a Bruker AXS "Nanostar" setup with a Cu Kα radiation source and pinhole collimation. The distance between sample and the 2D-detector was 24 cm. 2D patterns were transformed into a 1D radial average of the scattering intensity. Thermal gravimetric analysis (TGA) was carried out using TGAQ500 (TA Instruments) at a scan rate of 10 °C min^{-1}. Dynamic scanning calorimetry (DSC) was carried out using DSCQ100 (TA Instruments) at a scan rate of 10 °C min^{-1} with a maximum temperature as determined by TGA. Phase behavior was studied by polarized light optical microscopy (PLM). An Olympus BX 50 optical microscope equipped with an Olympus C-5060 wide zoom digital compact camera was used. Temperature-dependent measurements were performed using a Linkam TP92 Heater with THMS 600 heating stage. TEM analysis was performed in bright-field mode using a JEOL 1200 EX electron microscope operating at 120 keV. Tapping mode and phase images were obtaining using a multimode atomic force microscope equipped with a Nanoscope V controller (Veeco Instruments Ltd., Santa Barbara, USA). Tap300Al cantilevers were used with a rotated monolithic silicon probe with a tip radius of ca. 10 nm and were obtained from Budget Sensors (Sofia, Bulgaria). Images were analyzed using Gwyddion, an open source software program for SPM images.

Results and Discussion

G4-Surfactant Liquid Crystals. K^+-G4-DiC_n materials (i.e., G4-DiC_n materials prepared in the presence of K^+ ions) were readily prepared in a stepwise fashion by assembly in aqueous solutions (see Experimental Section). The precipitates were gel-like and could be dried under vacuum and dissolved in chloroform. Solvent casting of the purified materials produced transparent liquid-like (K^+-G4-DiC_{10} and K^+-G4-DiC_{12}) or waxy (K^+-G4-DiC_{14} and K^+-G4-DiC_{16}) thin films. In each case, energy-dispersive X-ray (EDX) analysis showed

(17) Kanie, K.; Nishii, M.; Yasuda, T.; Taki, T.; Ujiie, S.; Kato, T. *J. Mater. Chem.* **2001**, *11*, 2875–2886.

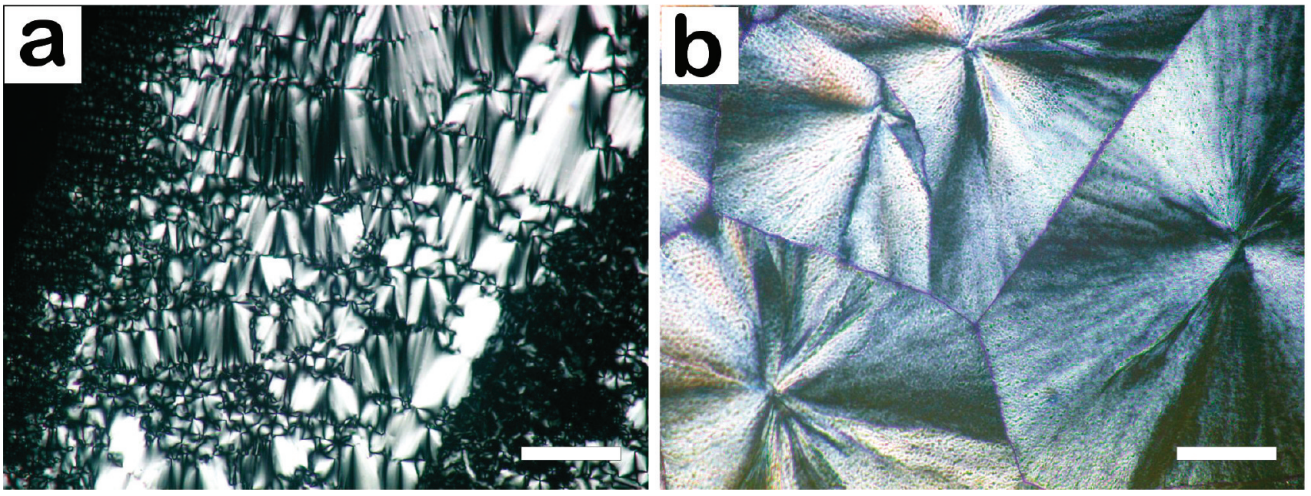

Figure 1. PLM micrographs of K^+-G4-DiC_{12} (left) and K^+-G4-DiC_{16} (right) recorded at room temperature (Scale bar = 50 μm). Textures for the K^+-G4-DiC_{10} and K^+-G4-DiC_{14} complexes were similar to that obtained for the K^+-G4-DiC_{12} sample. The appearance of the K^+-G4-DiC_{16} image (very sharp boundary edges) is indicative of a crystalline material.

the presence of potassium (3.3 keV) and phosphorus (2.0 keV), and thermogravimetric analysis (TGA) gave a degradation temperature of ca. 200 °C.

Differential scanning calorimetry (DSC) showed transitions in K^+-G4-DiC_{14} and K^+-G4-DiC_{16}, indicating that these samples were crystalline at room temperature (see the Suporting Information). In contrast, the K^+-G4-DiC_{10} and K^+-G4-DiC_{12} soft gels showed no transitions in the DSC curves. However, polarized light microscopy (PLM) indicated that all the K^+-G4-DiC_n materials were highly birefringent (Figure 1), thus indicating anisotropic molecular organization.

To elucidate the supramolecular organization and phase behavior of the anisotropic dGMP-based materials, we employed both wide-angle (WAXS) and small-angle X-ray scattering (SAXS) analyses, performed at room temperature. WAXS analyses clearly showed a reflection at ca. 0.33 nm ($2\theta = 27°$, see arrow in Figure 2a) that is characteristic of π-stacking of the guanosine bases as reported previously in synthetic systems and natural DNA G-quartet−containing systems.[18] Significantly, no sharp reflections were recorded in the wide-angle region for the K^+-G4-DiC_{10} and K^+-G4-DiC_{12} samples, but rather only a broad halo. Such a scattering pattern is typical for a liquid-like arrangement of alkyl chains. The results were therefore consistent with the formation of room-temperature thermotropic liquid crystals (see the Supporting Information for detailed EDX, TGA, DSC, and PLM data for all the prepared complexes). However, for both the K^+-G4-DiC_{14} and K^+-G4-DiC_{16} systems, sharp reflections were observed in their WAXS patterns, indicating crystalline phases at room temperature (see Figure 2a). SAXS analyses of the series of K^+-G4-DiC_n materials showed a gradual increase in the *d*-spacing of the repeating structures from 3.85 nm (K^+-G4-DiC_{10}), 4.0 nm (K^+-G4-DiC_{12}), 4.1 nm (K^+-G4-DiC_{14}) to 4.23 nm (K^+-G4-DiC_{16}) (Figure 2b).

(18) Parkinson, G. N.; Lee, M. P. H.; Neidle, S. *Nature* **2002**, *417*, 876–880.

Close inspection of the scattering patterns revealed the presence of 2D rectangular columnar phases in the K^+-G4-DiC_{14} and K^+-G4-DiC_{16} systems with lattice parameters of $a = 4.10$ nm and $b = 2.8$ nm, and $a = 4.23$ nm and $b = 3.4$ nm, respectively. In the case of both K^+-G4-DiC_{10} and K^+-G4-DiC_{12}, SAXS analyses showed the presence of two coexisting phases, with the majority phase being columnar.

Although the second phase was possibly columnar, the superposition of reflections did not allow for unambiguous determination. For instance, a columnar-rectangular structure of ca. 3.8 nm × 3.2 nm and a second phase indexed to a columnar structure with lattice constants of ca. 4.6 × 3.9 nm were identified for K^+-G4-DiC_{10}. Clearly, the presence of columnar phases in the K^+-G4-DiC_n materials is consistent with the formation of metal-ion intercalated G-quartet-based stacks. Moreover, these are complexed and plasticized by the alkyl tails associated with surfactant molecules bound at the available anionic phosphate sites to yield stable liquid-crystalline columnar structures. As a consequence, the increase in the length of the alkyl chains results in larger *d* spacings in the mesostructured phases.

TEM and AFM investigations confirmed the existence of the proposed columnar mesophase structures in all the K^+-G4-DiC_n materials (Figure 3 a−d). Uranyl acetate negatively stained TEM images of drop-cast samples showed well-ordered columnar structures (seen side-on) of several micrometers in length. The spacing between the regular columnar features measured from TEM images showed the width to be ca. 3 nm in all cases, with the high contrast sections increasing from 1.6 to 2 nm with an increase in the tail length. These values (4.6 to 5 nm for the DiC_n series) match the *d*-spacings obtained from SAXS analyses, especially given the different sample preparation methodologies. EDX analysis showed the presence of phosphorus and potassium at a ratio of ca. 3.5−4:1 in all cases and was generally consistent with the molar ratio of 4 dGMP to 1 K^+ in the G-quartet structure, thus

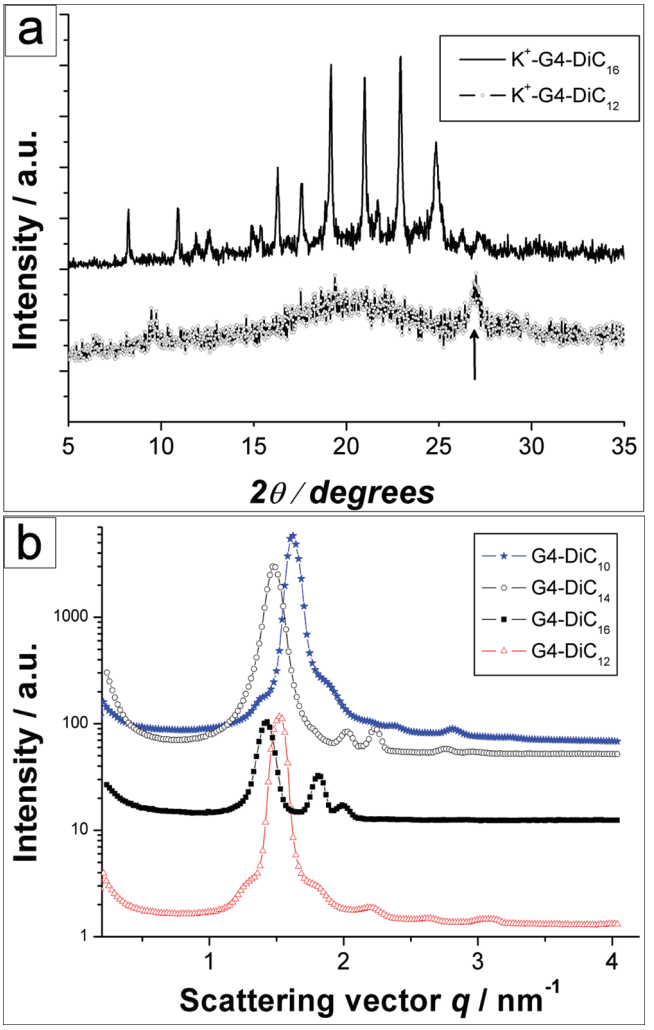

Figure 2. (a) WAXS data of K^+-G4-DiC_{12} (lower profile) showing a sharp reflection at 0.33 nm attributed to π-stacking (arrow), and general lack of crystallinity in the wide-angle region; corresponding data for K^+-G4-DiC_{16} showing a high degree of crystallinity (upper profile); (b) SAXS data for a series of K^+-G4-surfactant materials showing a gradual increase in the *d*-spacing with increasing chain length. See the text for more details.

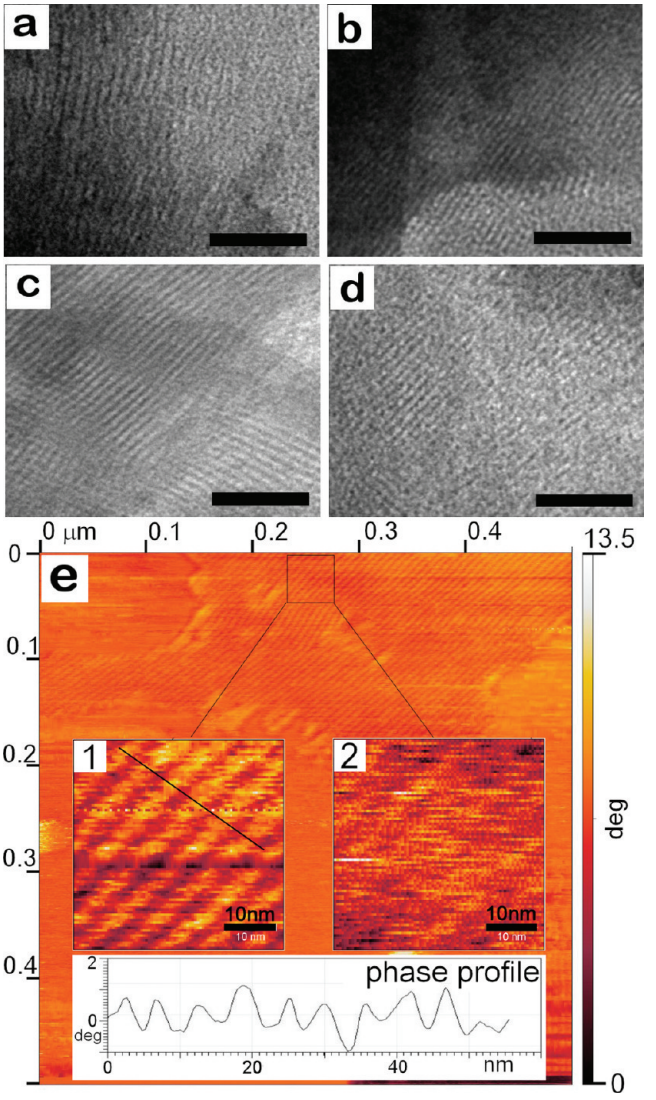

Figure 3. (a–d) TEM micrographs of uranyl-acetate stained K^+-G4-surfactant complexes confirming the columnar structures observed by SAXS analyses. (a) K^+-G4-DiC_{10}, (b) K^+-G4-DiC_{12}, (c) K^+-G4-DiC_{14}, (d) K^+-G4-DiC_{16} complexes (scale bars = 50 nm in all cases). (e) AFM phase contrast image of the K^+-G4-DiC_{12} complex showing a thin film of columns. Inset 1 is an enlarged phase contrast image showing the columnar structure (also see the phase profile) and inset 2 is the corresponding height image showing the height contrast of the columns. See text for more details.

indirectly supporting the formation of the G-quartet. Unstained TEM images showed a similar striped pattern, but with the features not as easily distinguishable as in the stained samples (see the Supporting Information).

AFM images, recorded in phase contrast mode, clearly showed the presence of columnar structures lying side-on across the mica substrate (Figure 3e). The width of the columns was ca. 7.5 nm, and the height of the individual columns determined to be 3 nm. The discrepancy with the dimensions obtained from TEM and SAXS was attributed to the presence of the hydrophilic mica substrate and effect of the AFM tip. Morphology mode images did not show any distinct features.

As the G-quartet motif is stabilized by metal cations through coordination from 8 oxygen atoms of two stacked G-quartet structures,[19] we utilized this molecular prearrangement as a means to include functional precursors into the well-ordered columnar structures. For this, we used Ag^+-G4-DiC_{12} as a model system for a proof-of-principle investigation into the use of such mesostructures as constrained nucleation and structure-directing environments for silver nanoparticle production.[20] G-quartet structures were prepared in the presence of Ag(I) ions in the absence of light. Complexation with the cationic DiC_{12} surfactant produced a white gel-like dispersion. To induce formation of Ag nanoparticles within the template, the materials were photoreduced by exposure to a low-powered UV source. No visible changes were observed after 2 h of exposure, with the samples exhibiting birefringence under cross polarizers. The textures

(19) Laughlan, G.; Murchie, A. I. H.; Norman, D. G.; Moore, M. H.; Moody, P. C. E.; Lilley, D. M. J.; Luisi, B. *Science* **1994**, *265*, 520–524.

(20) Ionic radius of 8-coordinated metal ions: K(I) 1.51 A, Ag(I) = 1.28A (, 88th Edition, 2007–2008). CRC Handbook of Chemistry and Physics, 88th ed.; CRC Press: Boca Raton, FL, 2007–2008.

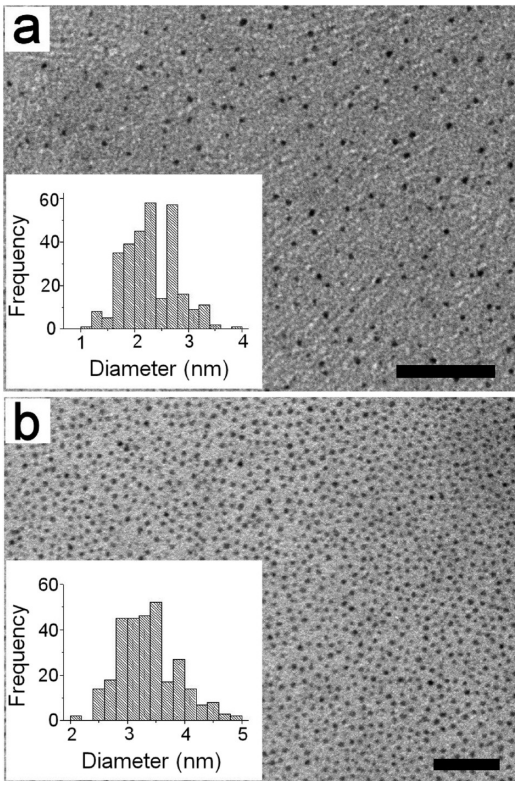

Figure 4. (a) TEM image of G-quartet-templated Ag nanoparticles distributed between the clearly visible columnar structures of the G4-DiC_{12} template (scale bar = 50 nm), particle diameter = 2.3 ± 0.5 nm. (b) The distribution of nanoparticles was not homogeneous on the TEM grid, but where concentrated, formed regular arrays as shown (scale bar = 50 nm), particle diameter = 3.4 ± 0.5 nm.

were similar to those found for the K^+-containing samples, the only difference being the presence of much smaller liquid crystal domains (see the Supporting Information for PLM images and further analytical data). After collecting, washing, and redissolving the material in dichloromethane or chloroform, TEM investigations (on drop-cast samples) showed the presence of discrete Ag nanoparticles organized either within the liquid-crystalline environment or in regular arrays on the TEM grid (Figure 4a and b, respectively). EDX confirmed the presence of small clusters of Ag, as shown by the particle size distributions in Figure 4. Selected-area electron-diffraction analysis gave powder diffraction ring patterns showing *d* spacings (*hkl* values) of 2.369 Å (111), 2.049 Å (200), 1.446 Å (220), 1.230 Å (311), and 0.904 Å (420), suggesting face-centered cubic Ag crystals (see the Supporting Information).

The narrow size distribution and small size of the nanoparticles can be attributed to preorganization of Ag(I) ions within the G-quartet structure. This constrained environment leads to a large number of localized nucleation centers that facilitate site-directed cluster formation and restricted crystal growth. This mechanism was consistent with the formation of ill-defined polydisperse Ag particles in the G-quartet matrix when the Ag(I) concentration was increased beyond the stoichiometric limit (see the Supporting Information for TEM micrographs of these control experiments).

In summary, we have demonstrated that complex functional nanomaterials based on stacked metal-ion-containing G quadruplexes and cationic surfactant self-assembly can be readily fabricated. Specifically, we showed that multiple noncovalent interactions can be utilized to construct well-organized thermotropic LC materials, which can be subsequently exploited for the production of complex materials comprising Ag nanoparticles. As further insight is gained into the binding capabilities and stabilities of such intricate structures, we expect this work to have significant impact on the development of new multifunctional guanosine-based liquid-crystalline materials, and contribute to the general understanding and utilization of the biologically relevant G-quartet motif in the realm of materials chemistry.

Acknowledgment. We thank the University of Bristol, EPSRC and DFG for financial support, and Ingrid Zenke (Max Planck Institute of Colloids and Interfaces, Germany) and Dr. Sergio Funari (DESY HASYLAB, Beamline A2) for technical support.

Supporting Information Available: Energy-dispersive X-ray (EDX) analyses, representative DSC and TGA data, selected area electron diffraction analysis of Ag nanoparticles, and TEM and WAXS results from control investigations (PDF). This material is available free of charge via the Internet at http://pubs.acs.org